X-641-70-395
PREPRINT

NASA TM X- 65393

INTRINSIC EFFICIENCIES OF SPHERICAL NaI(Tℓ) DETECTORS

J. I. TROMBKA

OCTOBER 1970

GSFC
GODDARD SPACE FLIGHT CENTER
GREENBELT, MARYLAND

14

PREPRINT

INTRINSIC EFFICIENCIES OF SPHERICAL NaI(Tl) DETECTORS

by

J. I. Trombka

Goddard Space Flight Center

August 1970

Goddard Space Flight Center

Greenbelt, Maryland

CONTENTS

Page

ABSTRACT v

1. Introduction 1

2. Construction of a spherical detector 2

3. Intrinsic detector efficiencies 2

4. Comparison of cylindrical and spherical detectors 7

5. Summary 10

References 10

ABSTRACT

The intrinsic efficiencies of spherical NaI(Tl) detectors are considered with respect to the efficiencies of cylindrical NaI(Tl) detectors. A simple method of calculating the intrinsic efficiencies of spherical detectors is presented. It is shown that the problems introduced by the dependence of detection efficiency on the angular distribution of the incident gamma-ray flux for cylindrical detectors can either be eliminated or greatly reduced by the use of spherical detectors.

INTRINSIC EFFICIENCIES OF SPHERICAL NaI(Tl) DETECTORS

by

J. I. Trombka

Goddard Space Flight Center

1. Introduction

A number of experiments employing NaI(Tl) detectors have been flown and are planned for future flights. In many of the experiments under consideration, a knowledge of the differential-energy photon spectrum is required. One measures the so-called pulse-height spectrum, which characterizes the interaction between the incident gamma-ray flux and the detector. There is not a one-to-one correspondence between the pulse-height and photon spectrum, but methods have been developed to infer the photon spectrum from the pulse-height spectrum[1-4]). In order to perform this analysis, the response functions and intrinsic efficiencies as functions of energy for the detection system must be known. Both functions depend on the angular distribution of the incident photon flux. The effects of this dependence can be greatly minimized and, in certain cases, can be completely eliminated if spherical detectors are used. Many problems in space flight gamma-ray spectroscopy involve the measurement of spectra wherein the angular distribution is completely unknown. Thus, it is extremely important that the effect of the angular distribution on the shape of the measured pulse height be minimized or eliminated.

The intrinsic detection efficiency for the detector system can be used to study the nature of the effects on the angular distribution of the incident evident flux and to show how these effects can be minimized with the use of spherical detectors.

2. Construction of a spherical detector

Because a spherical detector configuration is uncommon, let us briefly consider the construction of a spherical detector. Fig. 1 shows the design of a spherical detector. The crystal is connected to the front surface of the photomultiplier tube by a lucite light pipe. The energy resolution obtained with the spherical detector may not be quite so good as that obtained with a cylindrical detector, because of the possible light loss due to the increase in the number of optical connections.

3. Intrinsic detector efficiencies

Various types of detection efficiencies are defined in this section. It must be remembered that only one pulse appears at the output of the photomultiplier tube for each gamma ray that interacts with the crystal. Fig. 2 shows a measured pulse-height distribution for the 0.835-MeV line of ^{54}Mn interacting with a 3″ × 3″ NaI(Tl) detector. The number of pulses produced, independent of pulse height and notwithstanding the effects of scattering from the surrounding media, will be equal to the number of primary collisions in the crystal. The total area A_T under a pulse-height spectrum, with scattering effects ignored, is equal to the total number of primary collisions[5]).

Let us now consider a point-source emitter of monoenergetic gamma rays for the following two cases: (a) a cylindrical detector and (b) a spherical detector (fig. 3). Then

$$A_T = I_0(\Omega/4\pi)(\epsilon_{Ti}) , \qquad (1)$$

where

I_0 is the intensity of the source;

$\Omega/4\pi$ is the fraction of solid angle subtended by the source and detector;

ϵ_{Ti} is the intrinsic efficiency of the detector. This is the probability that, if a gamma ray strikes the crystal, it will interact with the crystal.

If any interaction in which a gamma ray produces a scintillation in the crystal is considered an absorption interaction, then the linear absorption coefficient μ can be defined as the probability that a gamma ray will undergo an absorption interaction along the path length ρ in the absorbing medium. The principal absorption interactions are (1) photoelectric absorption, (2) Compton scattering, and (3) pair production. The total absolute intrinsic efficiency ϵ_{Ta} can then be defined as

$$\epsilon_{Ta} = \int_{\text{over } \Omega} \{1 - \exp(-\mu\rho)\} d\Omega/4\pi \, . \tag{2}$$

This is the probability that a gamma ray emitted from the source will interact at least once with the crystal. The total intrinsic efficiency ϵ_{Ti} can be defined in terms of ϵ_{Ta} as

$$\epsilon_{Ti} = \epsilon_{Ta} / \left(\int_{\text{over } \Omega} d\Omega/4\pi \right) . \tag{3}$$

The total intrinsic efficiency is thus related to the angular distribution of the incident flux, as shown in eq. (3). It is this property that we wish to study. As a first step, we study ϵ_{Ti} as a function of the energy and distance of a point source from the top of the detector. Values of ϵ_{Ta} as a function of source-crystal geometry for right cylindrical crystals and beveled right cylindrical crystals have been calculated[6-8]). In the following, we will develop a simple numerical method for solving eq. (3) for spherical detectors. From fig. 3b,

$$\Omega/4\pi = \tfrac{1}{2}(1 - \cos\theta_{max}) . \tag{4}$$

Let

$$\beta = h + a , \tag{5}$$

where h is the height above the crystal and a is the crystal radius, and

$$\rho = 2(a^2 - \beta^2 \sin^2\theta)^{\frac{1}{2}} . \tag{6}$$

Then eq. (4) becomes

$$\Omega/4\pi = \tfrac{1}{2}[1 - \{(\beta^2 - a^2)/\beta^2\}^{\frac{1}{2}}] . \tag{4a}$$

Now, let $h = ma$, that is, the height from the top of the crystal will be measured in units of the radius a. Eq. (4a) now becomes

$$\Omega/4\pi = \tfrac{1}{2}[1 - \{1 - 1/(m+1)^2\}^{\frac{1}{2}}] . \tag{4b}$$

We now define

$$\gamma^2 = \{1 - 1/(m+1)^2\} \tag{7}$$

and $d = 2a$, the crystal diameter. With these definitions, the intrinsic efficiency can be written as

$$\epsilon_{Ti} = 1/(1-\gamma) \int_0^d \mu \exp(-\mu\rho)[1 - \{\gamma^2 + \rho^2/d^2(m+1)^2\}^{\frac{1}{2}}]d\rho . \tag{8}$$

An exact solution can be found for $m = 0$ and $m \to \infty$; the latter case is the parallel beam solution. For $m = 0$,

$$\epsilon_{Ti0} = \int_0^d \mu \exp(-\mu\rho)(1 - \rho/d)d\rho$$

$$= 1 - \{1 - \exp(-\mu d)\}/\mu d . \tag{9}$$

For $m \to \infty$,

$$\epsilon_{Ti\infty} = \int_0^d \mu \exp(-\mu\rho)(1 - \rho^2/d^2)\,d\rho$$

$$= 1 - 2\{1 - \exp(-\mu d)\}/(\mu d)^2 + 2\exp(-\mu d)/\mu d\,. \tag{10}$$

For the other cases, the definite integral cannot be evaluated. Consider the following factor in the integral of eq. (8):

$$F_m = \{1/(1-\gamma)\}[1 - \{\gamma^2 + \rho^2/d^2(m+1)^2\}^{1/2}]\,. \tag{11}$$

For a good approximation, it has been found that

$$F_m \simeq \sum_{l=0}^{4} a_{lm}(\rho/d)^l\,. \tag{12}$$

The values of a_{lm} can be found for various values of m and ρ/d. These results are independent of the crystal diameter d and the type of material (i.e., the linear absorption coefficient). Some results of the a_{lm} calculation are shown in table 1.

Substitution of eq. (12) in eq. (8) and use of the definition

$$I_0 = \{1 - \exp(-\mu d)\}$$

yield

$$I_n = (nI_n - 1)/\mu d - \exp(-\mu d) \tag{13}$$

for $n > 0$.

Equation (8), after integration, reduces to

$$\epsilon_{Ti} = \sum_{l=0}^{4} a_{lm} I_l\,. \tag{14}$$

Table 1

Values of a_{lm} for various values of m (the relative height as a multiple of crystal radius) and ρ/d (the ratio of the path length in the crystal to the crystal diameter).

l	ρ/d	a_{lm}							
		$m = 0$	$m = 0.05$	$m = 0.1$	$m = 0.2$	$m = 0.5$	$m = 1.0$	$m = 2.0$	$m = \infty$
0	0	1.0	1.0	1.0	1.0	1.0	1.0	1.0	1.0
1	¼	−1.0	0.050310	0.025523	0.025523	0.008280	0.000508	0.000244	0
2	½	0	−2.488485	−1.638707	−1.638707	−1.240919	−1.088209	−1.03268	−1.0
3	¾	0	2.186250	0.748565	0.748565	0.195392	0.038016	0.006816	0
4	1	0	−0.748075	−0.135381	−0.135381	0.037247	0.049685	0.025621	0

Calculations were carried out for spherical NaI(Tl) detectors 3.44 in. in diameter. The 3.44-in. sphere had the same volume as a 3″ × 3″ right cylindrical NaI(Tl) detector.

4. Comparison of cylindrical and spherical detectors

As was mentioned above, the variations of the intrinsic efficiency as a function of the angular distribution of the incident flux can be studied by considering the variations in ϵ_{Ti} as a function of the distance to a point source along the axis and above a cylindrical crystal, a beveled cylindrical detector, and a spherical crystal. A cylindrical NaI(Tl) detector, 3 in. high and 3 in. in diameter, is compared with a spherical NaI(Tl) detector, 3.44 in. in diameter. The two detectors have the same active volume. Fig. 4 shows the results obtained when an incident beam of 2.04-MeV gamma rays is used. Table 2 is a compilation of values of ϵ_{Ti} for a 3.44-in.-diameter spherical crystal as a function of energy and source-to-crystal distance. From fig. 4 and table 2 it can be seen that, after the source has been moved to distances greater than one-half the diameter of the sphere, the efficiency is within 5 percent of the parallel-beam case. If we consider the 3″ × 3″ right cylinder, the intrinsic efficiency at 70 cm is still 7 percent less than the parallel-beam case. In fact, it is not until the point source is 100 cm or farther from the surface of the right cylinder along the axis of the cylinder that the efficiency is within 5 percent of the parallel-beam case. The short path lengths that are due to the edges of the right cylinder detector greatly influence the variations in the intrinsic efficiency. When the point source is on the top of the crystal, one does not, in a sense, "see" the short paths at the corners of the cylinder. As the point moves away from the top of the cylinder, one sees the short paths at the corners of the cylinder, and the intrinsic efficiencies decrease to some minimum value. When these corners become less significant as the paths move further from the top of the crystal, the efficiency starts

Table 2

Intrinsic efficiencies as functions of energy and distance for a sphere 3.44 in. in diameter.

Energy	$m = 0$	$m = .001$	$m = .005$	$m = .01$	$m = .05$	$m = 0.1$	$m = 0.2$	$m = 0.5$	$m = 1.0$	$m = 2.0$	∞
0.105	0.977	0.983	0.989	0.992	0.999	0.999	0.999	0.999	0.999	0.999	0.999
0.129	0.962	0.971	0.979	0.984	0.996	0.996	0.996	0.997	0.999	0.999	0.997
0.152	0.943	0.957	0.970	0.979	0.996	0.996	0.996	0.997	0.997	0.997	0.997
0.212	0.886	0.902	0.920	0.930	0.957	0.961	0.966	0.970	0.972	0.973	0.974
0.332	0.774	0.794	0.815	0.828	0.865	0.873	0.884	0.894	0.898	0.901	0.902
0.566	0.646	0.665	0.685	0.698	0.737	0.748	0.760	0.774	0.780	0.783	0.786
1.10	0.528	0.544	0.562	0.573	0.609	0.620	0.633	0.646	0.653	0.656	0.659
2.04	0.443	0.451	0.473	0.483	0.514	0.524	0.536	0.549	0.554	0.559	0.561
3.8 and 7.9	0.402	0.416	0.430	0.439	0.469	0.478	0.490	0.502	0.507	0.511	0.513
5.5	0.396	0.409	0.423	0.432	0.461	0.471	0.482	0.494	0.500	0.503	0.506

increasing. When the distance to the point source approaches infinity, the parallel beam cases, the corner effects are completely eliminated.

The extent of this corner effect can be shown by calculation of the intrinsic efficiency as a function of distance from the top of a beveled cylindrical crystal for which some of the edge effects have been removed. The results of this calculation are also shown in fig. 4. The intrinsic efficiencies do not decrease as fast for small source-to-detector distances as they do for the right cylindrical crystal, and they start to approach the parallel-beam case with the point source closer to the top of the crystal than is the case with the right cylindrical crystal. The distance required to approach the parallel-beam case is still much greater than is the case with the spherical crystal.

We now look at the case of isotropic fluxes. It may be assumed that an isotropic flux can be simulated by calculating the intrinsic efficiencies for a parallel beam and integrating over all possible angles of incident flux. For the spherical crystal, the parallel-beam intrinsic efficiency is independent of the angle of incidence. Thus, the isotropic flux and parallel-beam intrinsic efficiency are the same.

We have not calculated the isotropic-flux intrinsic efficiency for a right cylindrical 3″ × 3″ detector, but the intrinsic efficiencies as functions of energy have been calculated for a 3″ × 3″ crystal with a parallel beam of gamma rays incident on the surface for two cases: parallel to the crystal axis and perpendicular to the crystal axis. These efficiencies and the efficiencies calculated for the 3.44-in. spherical crystal are compared in fig. 5. The intrinsic efficiencies for the spherical crystal lies between those for the two cylindrical-crystal cases. The maximum ϵ_{Ti} for the cylindrical crystal occurs when the beam is parallel to the axis of the cylinder. The values of the intrinsic efficiencies when the beam is perpendicular to the axis are smaller than those for the spherical crystal which had the same volume.

These values may not be the minimum for the cylinder but they should be close to the minimum. Thus, the average obtained by integration over all possible angles of incidence would yield the intrinsic efficiency for the isotropic case and should lie somewhere between the two cases for cylindrical crystals shown in fig. 5.

Experimental measurements have also been made with a 2-in. spherical crystal[9]). The results of these measurements are consistent with those properties of spherical crystals described above.

5. Summary

The above arguments and calculations should indicate the strong dependence of the detection efficiencies for cylindrical crystals on the angular distribution of the incident gamma-ray flux. This dependence can be greatly minimized by the use of spherical crystals. Also, since the parallel-beam case and the isotropic-flux case are the same for spherical crystals, many properties of the spherical crystals (e.g., peak-to-total response functions) can be measured with parallel-beam geometry, a much easier experimental procedure.

In space-flight applications, where one cannot precisely define the angular distribution of the incident gamma-ray flux, or in those cases where one is measuring isotropic distribution, the spherical detector may be rather useful. In fact, in these cases, because of the properties of spherical crystals, one can most easily infer the true photon spectrum from an analysis of the pulse-height spectrum.

References

[1]) J. I. Trombka and R. L. Schmadebeck, A method for the analysis of pulse-height spectra containing gain-shift and zero-drift compensation, Nucl. Instr. and Meth. 42 (1966) 253.

[2]) J. I. Trombka, Interpretation of cosmic X-ray and gamma ray spectra, Nature 226 (1970) 827.

[3]) J. I. Trombka, F. Senftle and R. L. Schmadebeck, Neutron radiative capture methods for surface elemental analysis, Nucl. Instr. and Meth. (to be published fall 1970).

[4]) I. Adler and J. I. Trombka, Data processing and analysis, Chapt. 5, *Geochemical exploration of the moon and planets* (Springer-Verlag, Heidelberg, Berlin, New York to be published October 1970).

[5]) P. R. Bell, The scintillation process in *Beta and gamma ray spectroscopy*, ed. Kai Sieghahn (North-Holland Publishing Co., Amsterdam, 1955).

[6]) W. F. Miller, J. Reynolds and W. J. Snow, Efficiencies and photofractions for gamma radiation on NaI(Tl) activated crystals, ANL-5902 (August, 1958).

[7]) S. H. Vegors, L. L. Marsden and R. L. Heath, Calculated efficiencies of cylindrical radiation detectors, IDO-16370 (September, 1952).

[8]) J. E. Francis, C. C. Harris and J. I. Trombka, Variation of NaI(Tl) detection efficiencies with crystal size and geometry for medical research, ORNL-2204 (February, 1957).

[9]) J. I. Trombka, On the analysis of gamma ray pulse height spectra, Dissertation (University of Michigan, 1962).

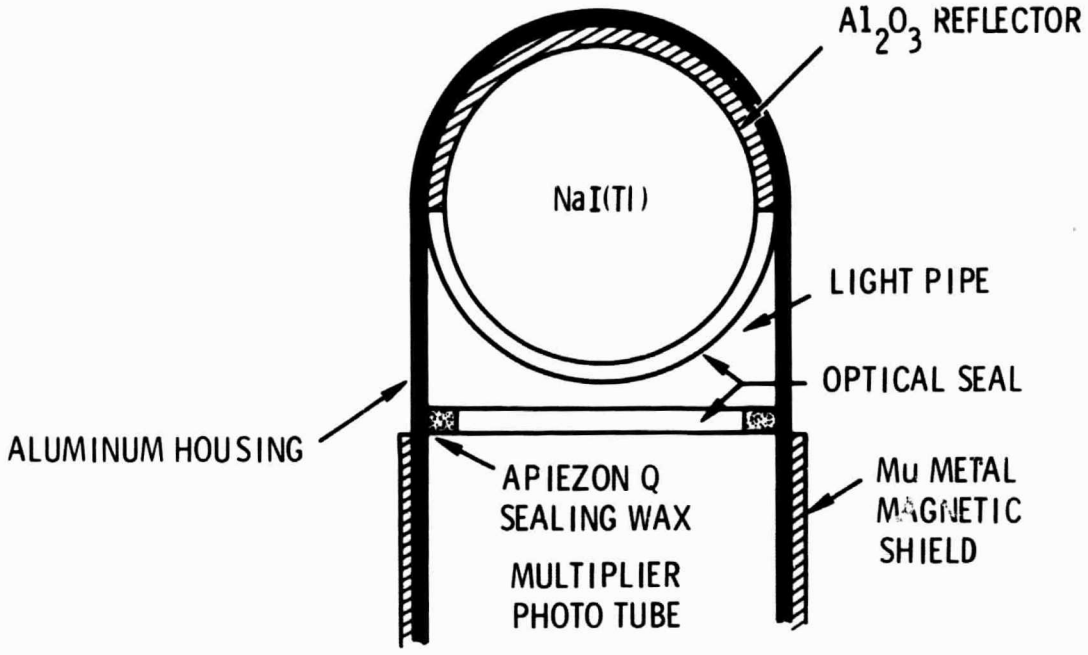

Fig. 1. Construction of the 2" spherical detector.

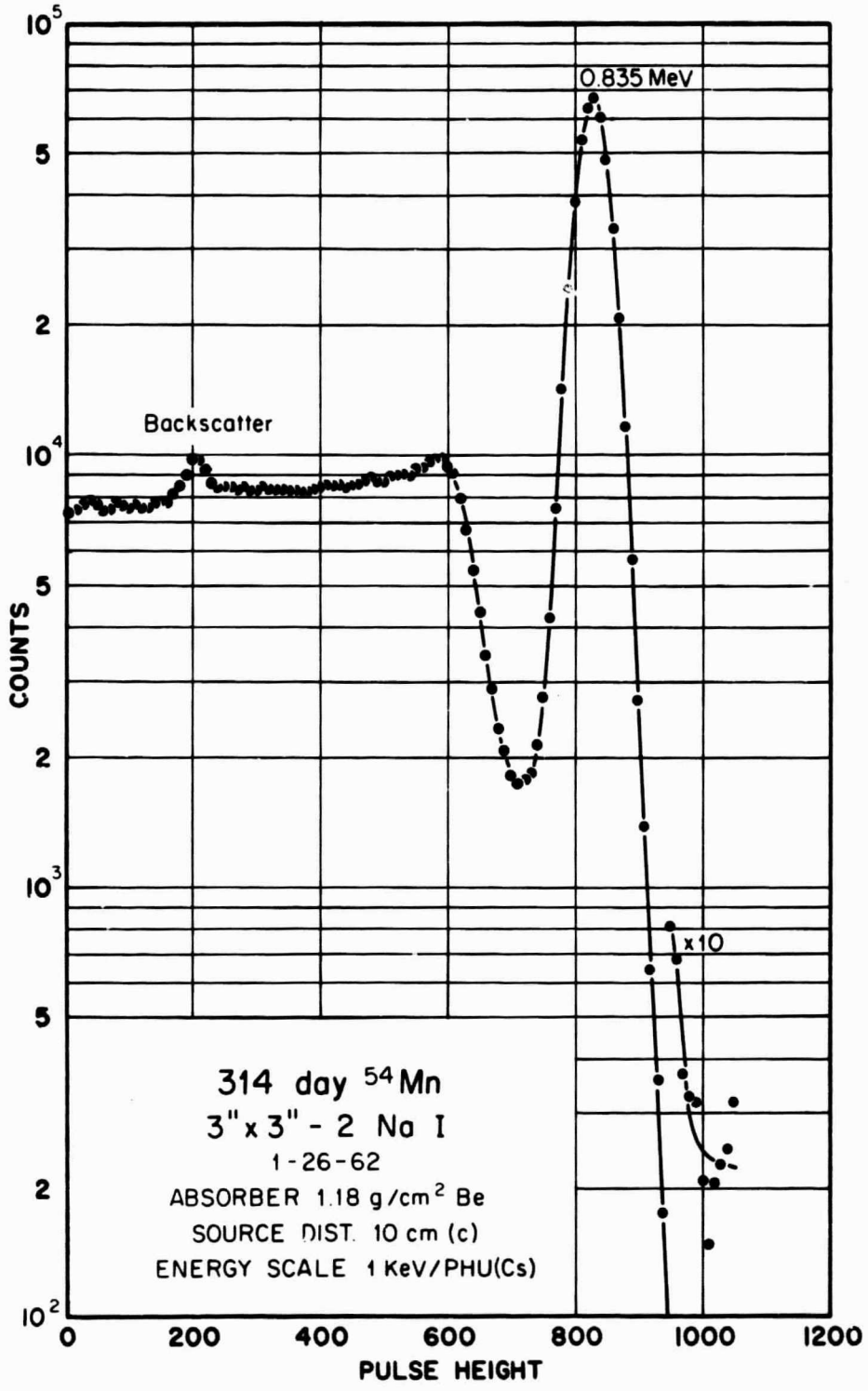

Fig. 2. Pulse-height spectrum for 0.835-MeV line of ^{54} Mn interacting with an NaI (Tl) detector.

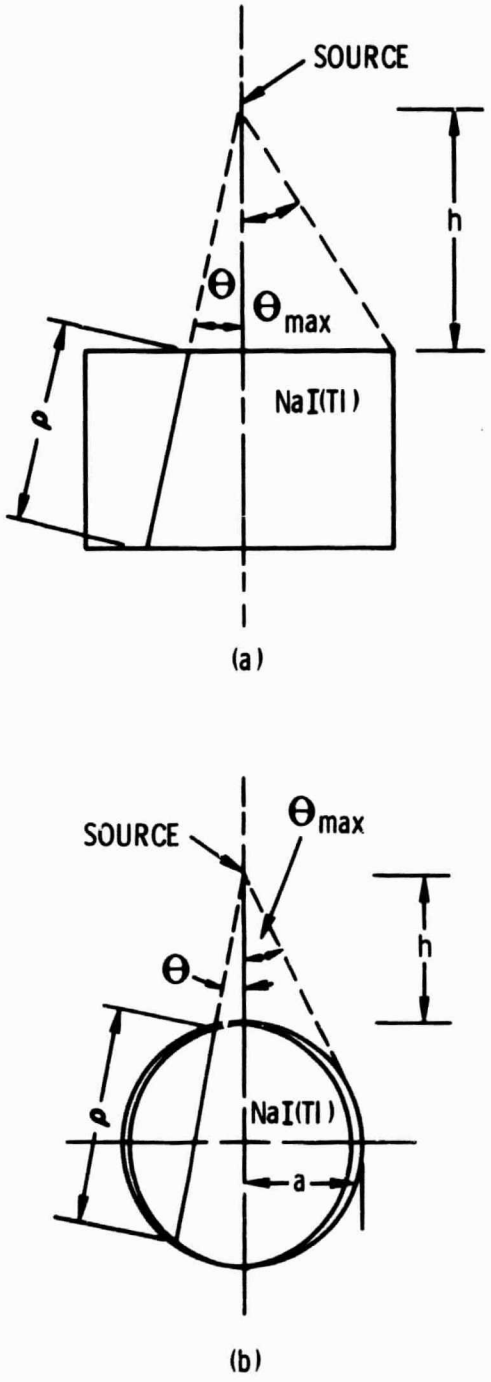

Fig. 3. Source detector geometry for (a) cylindrical crystal and (b) spherical crystal.

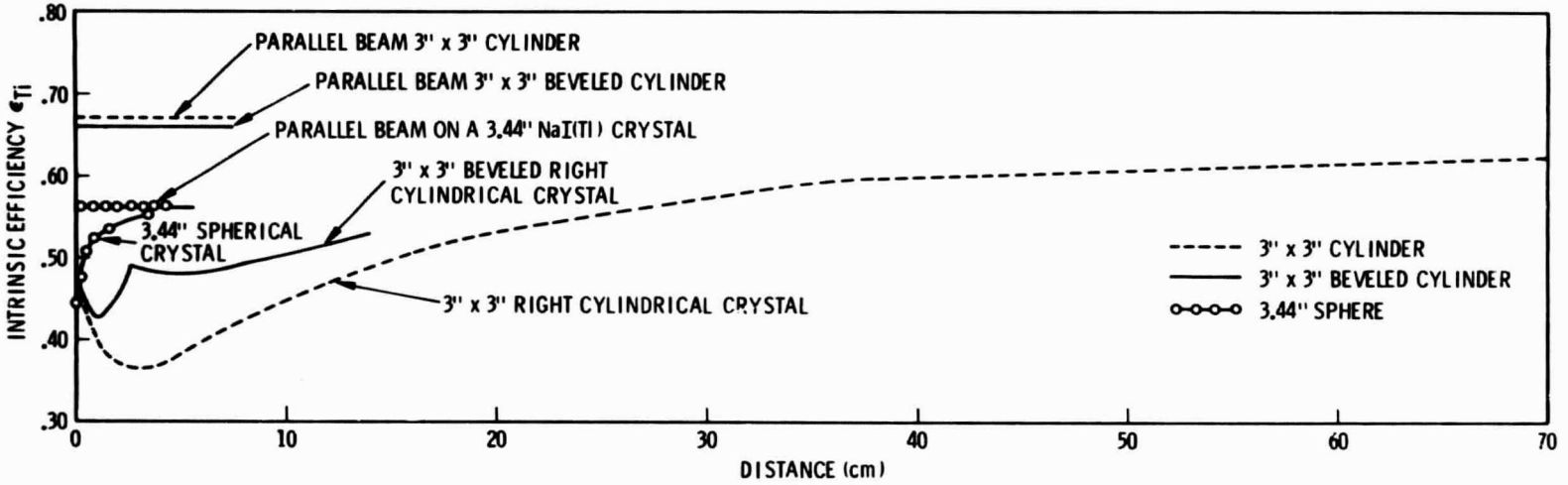

Fig. 4. Intrinsic efficiency as a function of distance for various crystals with 2.04- MeV gamma rays.

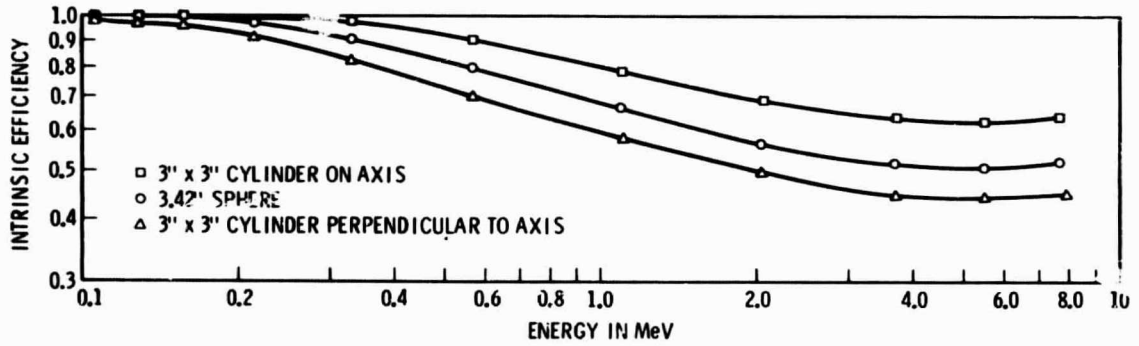

Fig. 5. Intrinsic efficiency as a function of energy for a parallel beam incident on various crystals.